



© Article authors. This is an open access article distributed under the Creative Commons Attribution-NonCommercial-NoDerivs license. (<http://creativecommons.org/licenses/by-nc-nd/3.0/>).

ISSN online 2545-2819

ISSN print 0800-6377

DOI: 10.2478/ncr-2018-0016

Received: Sept. 14, 2018

Revision received: Nov. 28, 2018

Accepted: Nov. 29, 2018

## Prediction of Restraint Moments in Precast, Prestressed Structures Made Continuous



Ulla Kytölä, M.Sc  
Ph.D. student  
Dept. of Civil Engineering, Tampere University of Technology  
Korkeakoulunkatu 5,  
FI-33720 Tampere  
E-mail: [ulla.kytola@tut.fi](mailto:ulla.kytola@tut.fi)



Anssi Laaksonen, D.Sc  
Professor  
Dept. of Civil Engineering, Tampere University of Technology  
Korkeakoulunkatu 5,  
FI-33720 Tampere  
E-mail: [anssi.laaksonen@tut.fi](mailto:anssi.laaksonen@tut.fi)

### ABSTRACT

This paper studies restraint moments developing in simple-span precast, prestressed beams made continuous. Methods of evaluating restraint moments produced by creep and differential shrinkage are presented. Shrinkage and creep properties of composite structures, beam and deck parts were tested and compared to values defined according to Eurocode models. Finally, the restraint moments were calculated with both material models for the two-span parking deck structure. The study confirmed the findings of previous studies: that the methods that are used overestimate the negative restraint moment produced by differential shrinkage.

**Key words:** Restraint moment, creep, differential shrinkage, continuity, prestressed concrete.

## 1. INTRODUCTION

Heavily loaded building structures and congested building sites are growing more common in Finland due to urbanisation. In many projects, single-span, simply supported precast prestressed beams are insufficient to carry the imposed loads, making cast-in-place (CIP) concrete the only alternative. There is a need in the construction field to determine ways to increase the application of precast prestressed concrete girders, which facilitates working phases on site.

It is common in many parts of the world to construct multi-span bridges composed of simple-span precast prestressed girders and CIP decks. Simple-span girders are made continuous with a CIP connection over the supports and by post-tensioning. In this method, the girders act as simple spans for dead loads before the connection is completed. After continuity is achieved, the composite section of the prestressed beam and CIP deck slab carry the superimposed dead and live loads as a continuous structure. Compared to simple-span girders, the advantages of girder continuity are reduced bending moments, improved accident and seismic performance, and a reduction in the amount of needed expansion joints, which require lots of maintenance.

There has been a considerable amount of research concerning bridges constructed in this way. Continuity of precast, prestressed girders is also used to some extent in building structures, but there is only little information available about the experience gained from those structures. At Tampere University of Technology (TUT), a research project founded by the Finnish Concrete Industry has begun to study the potentials of simple-span precast, prestressed concrete girders made continuous in building structures with heavy loads.

Prestressed girders have a tendency to exhibit camber after prestress transfer due to the effect of creep. If the element is simply supported, the ends of it will rotate because of creep and no external loads are developed. When simply supported beams are connected together, their ends are restrained from any rotation; because of that, a positive restraint moment develops at the intermediate support. In this type of element girder – in-situ-slab composite structure the slab is cast after the girders. When the slab is cast, the girders have already had time to shrink and there is less shrinkage left, whereas the slab's shrinkage has only started. This strain difference between the slab and the girder is called differential shrinkage, and it is presumed to cause downward deflection to the composite structure. This movement is restrained in the structure's continuous supports, which causes negative restraint moment to the structure. The final restraint moment is the sum of the effect of creep and differential shrinkage, and it can be positive or negative. Temperature difference also produces restraint moments in statically indeterminate structures. Usually heavily loaded building structures have sufficient thermal insulation to prevent strong temperature variation caused by outdoor conditions. Hydration heat of the in-situ-deck concrete might still produce variations in the temperature distribution of the structure during the first few days after the casting [1]. Restraint moments caused by these temperature changes are not included in this paper.

EN1992-1-1 provides methods to evaluate creep and shrinkage. The amount and developing rate of creep and shrinkage can vary widely, and the value calculated with Eurocode methods may differ considerably from real strains. Because of this, many references recommend material testing of the concrete in question beforehand in order to obtain a more accurate analysis about restraint moments in the design phase [2, 3]. Evaluating restraint moments in the structure is important because they affect the continuity of the structure. If the positive restraint moment exceeds the cracking moment of the connection continuity may be lost. The positive restraint moment increases the tensile stresses of soffits in the span, whereas the negative moment adds

compression stresses to the soffits at the intermediate support. These effects should be taken into consideration in stress limitation checks and other SLS design, which normally controls the design of prestressed building structures in heavy exposure classes [3, 4, 5, 6].

## **2. RESEARCH OBJECTIVE**

This paper is a part of doctoral research, which focuses on extending the application of precast, prestressed concrete beams with continuity. The objective of this paper and the first phase of the study is to concentrate on time-dependent restraint moments of these kinds of structures. Following phases will concentrate on the properties and function of continuity connection between precast girders in different states. Furthermore, complete  $\frac{1}{2}$ -scale continuous two-span composite girders will be constructed, tested and analysed.

The majority of the earlier research studies the problem from the standpoint of bridge girders made continuous. Dimensions and cross-sections differ from each other in building and bridge structures. The aim is to study the matter from the building structure point of view and estimate the magnitude of restraint moments.

The time-dependent properties of concrete have significant influence on restraint moments. It is recommended that tests should be conducted beforehand to evaluate true time-dependent strains [2,7]. In an experimental study, the properties of creep, shrinkage and elastic modulus were measured in typical types of Finnish concrete used in precast, prestressed elements and CIP slabs. An analytical tool was developed to evaluate restraint moments in simple-span girders made continuous. A representative composite two-span parking deck structure was selected for use as an example structure and studied. The calculation is made with two different material properties which are measured and defined according to EN 1992-1-1.

## **3. BACKGROUND**

### **3.1 Shrinkage and creep**

Shrinkage consists of drying and autogenous shrinkage. Drying shrinkage denotes the reduction in volume resulting from a loss of water. Contrary to drying shrinkage, autogenous shrinkage doesn't involve moisture transition. It is the result of chemical shrinkage affiliated with the hydration of cement particles. The magnitude of shrinkage depends on the mix design, size and shape of the structure, relative humidity and concrete curing. EN1992-1-1 provides analytical formulas for predicting mean values for autogenous and drying shrinkage strain. The variance of shrinkage is assumed to be  $\pm 30\%$ . The shrinkage strain is assumed to be constant within the cross section.

When concrete is loaded, it undergoes both elastic and viscous deformation. Elastic deformation happens quickly and the concrete returns to its original state once the load is removed. On the other hand, viscous deformation increases slowly with time as the concrete experiences a sustained load. This viscous property of concrete is called creep. The amount and developing rate of creep are influenced by aggregate, cement type, used additives, water-cement ratio, aggregate-cement ratio, the age of the concrete when first load is applied, duration and magnitude of load, temperature, relative humidity, size and shape of the structure, and concrete

curing [8]. Creep is usually described by means of a creep coefficient which is defined as the ratio of the given creep strain to the initial elastic strain. EN 1992-1-1 provides analytical formulas for predicting the development of the creep coefficient. The variance of creep is assumed to be  $\pm 20\%$  [9].

Most of the things mentioned above can be taken into account in Eurocode equations when predicting creep and shrinkage, but there are also things that are disregarded. In Finland, the majority of prestressed concrete elements are manufactured from self-consolidating concrete (SCC), which has a high paste content. Because of this, SCC creeps and shrinks about 10-20% more compared to ordinary concrete according to studies. This is left out in the Eurocode equations on the basis that the strains are still within the variance mentioned earlier [2,9].

### 3.2 Strain under constant stress [2]

In the Effective Modulus Method (EMM), long-term deformations are calculated based on the effective modulus of elasticity of concrete, which can be calculated with Eq. (1).

$$E_{c,eff}(t, t_0) = \frac{E_{cm}(t_0)}{1 + \frac{E_{cm}(t_0)}{E_{cm}} \varphi(t, t_0)} \quad (1)$$

where

$E_{cm}(t_0)$	is the modulus of elasticity at the time of loading $t_0$
$E_{cm}$	is the modulus of elasticity at the age of 28 days
$\varphi(t, t_0)$	is the creep coefficient

Creep compliance function is the inverse of effective modulus of elasticity (Eq. (2)). Time-varying strains in concrete can be calculated by multiplication of the known stress and compliance function  $\varnothing(t, t_0)$ .

$$\varnothing(t, t_0) = \frac{1}{E_c(t_0)} + \frac{\varphi(t, t_0)}{E_c(28)} \quad (2)$$

Strain  $\varepsilon_c(t, t_0)$  of concrete at time  $t$  for constant compressive stress  $\sigma_0$  applied to the concrete at the concrete age  $t_0$  including shrinkage  $\varepsilon_s(t)$  is

$$\varepsilon_c(t, t_0) = \sigma_0 \varnothing(t, t_0) + \varepsilon_s(t) = \sigma_0 \left( \frac{1}{E_c(t_0)} + \frac{\varphi(t, t_0)}{E_c(28)} \right) + \varepsilon_s(t) \quad (3)$$

### 3.3 Strain under time-dependent stress

Concrete exhibits ageing. As time passes, concrete stiffness increases and creep rate decreases. If strains caused by time-dependent stress are predicted with EMM, the results are incorrect. EMM doesn't take into account that (because of the ageing of concrete) later strains are less than those that would be generated if the same stress change happened right after first loading [10,11]. The theory of linear creep is based upon the principle that time-dependent stress can be taken into account in creep calculations with the principle of superposition. In this step-by-step method, change in the constantly varying stress is divided into small increments. These increments can be superimposed considering their time of duration and the maturity of the

concrete. Using the principle of superposition, the strain of concrete at time  $t$  for small increments of stress can be computed with Equations (4) and (5) [9, 12, 13, 14, 15].

$$\varepsilon_c(t, t_0) = \sigma_0 \left( \frac{1}{E_c(t_0)} + \frac{\varphi(t, t_0)}{E_c(28)} \right) + \int_{\tau=t_0}^t \frac{\partial \sigma(\tau)}{\partial \tau} \cdot \left[ \frac{1}{E_c(\tau)} + \frac{\varphi(t, \tau)}{E_c(28)} \right] d\tau + \varepsilon_s(t) \quad (4)$$

$$\varepsilon_c(t, t_0) = \sigma_0 \left( \frac{1}{E_c(t_0)} + \frac{\varphi(t, t_0)}{E_c(28)} \right) + \sum_{i=1}^n \left( \frac{1}{E_c(t_i)} + \frac{[\varphi(t, t_i)]}{E_c(28)} \right) \Delta \sigma(t_i) + \varepsilon_s(t) \quad (5)$$

It is difficult to find a solution to these equations because of the complicated mathematical form of the creep function. In 1967, Trost separated an ageing function from the creep function and developed a simpler equation to predict time-dependent stress-strain relation (Eq. (6)) [10, 16, 22].

$$\varepsilon_c(t, t_0) = \frac{\sigma_0}{E_c(t_0)} + \varphi(t, t_0) \frac{\sigma_0}{E_c(28)} + \frac{\sigma(t) - \sigma_0}{E_c(28)} \left( \frac{E_c(28)}{E_c(t_0)} + X \varphi(t, t_0) \right) + \varepsilon_s(t) \quad (6)$$

This method, called the Age-Adjusted Effective Modulus Method (AAEMM), is based on superposition and the observation made by Trost that the variation of the ageing function is only minor after first loading [12, 17]. Because of that, the ageing function can be taken in simplified calculations as a time constant. This constant value is called ageing coefficient  $X$ , and it depends on creep coefficient, time of first loading and the load duration. Values and graphs of the ageing coefficient are presented in many references [11, 15, 18]. The ageing coefficient value varies between 0.5 and 1. When the time of loading is early,  $X$  is near 0.5, whereas the coefficient tends to be near 1 at later loading. Extensive investigations concerning the ageing coefficient value have been conducted, and according to a statement by Trost one can determine an ageing coefficient of  $X = 0.8$  when the usual load carrying age  $t_0$  is between 3 and 90 days and typical values of final creep coefficient are between 1 and 4 [15].

According to many researchers, this is the most accurate simplified method for analysing the time-dependent effects of concrete structures. There are errors in creep prediction models and in the linear model itself. Because of that, the gain in accuracy achieved by the more refined linear methods is often fictitious [11, 19, 20]. Similar to EMM, Trost's method is also based on elastic analysis with a modified elastic modulus called the age-adjusted modulus of elasticity (Eq. (7)).

$$E_{c,adj}(t, t_0) = \frac{E_{cm}(t_0)}{1 + \frac{E_{cm}(t_0)}{E_{cm}} X \varphi(t, t_0)} \quad (7)$$

Now Eq. (6) may be written in the following simple form [18]

$$\varepsilon_c(t, t_0) = \frac{\sigma_0}{E_{c,eff}(t, t_0)} + \frac{\sigma(t) - \sigma_0}{E_{c,adj}(t, t_0)} + \varepsilon_s(t) \quad (8)$$

### 3.4 Restraint moment due to change in the static system

Creep and applied loads cause no time-dependent restraint moments in statically indeterminate structures that are homogenous and monolithically built. Structures deform but their internal forces do not change as long as the support conditions remain unchanged [11, 21].

When a simple-span structure is made continuous, the structure's restraint conditions are modified after the application of prestress force and self-weight of the structure. A modification of restraint conditions produces time-dependent variation of the initial elastic stresses and restraint reactions. Creep will tend to cause support reactions built up from staged construction to redistribute towards the support reactions that would have been produced if the structure had been constructed monolithically [22]. The effect of creep redistribution is illustrated in Fig. 1. Variance of the total moment is presented on the left hand side of the figure, while pure restraint moment is displayed on the right. In the upper part of Fig. 1, the effect of creep is illustrated for the dead load moments of two simple-span beams made continuous at time  $t = t_0$ .

- 1) At time  $t = t_0$ , the moment is distributed span-by-span and the moment is  $M_0$  (continuous line)
- 2) If the structure was constructed monolithically the moment would be  $M_1$  (dashed line)
- 3) When the structure is made continuous afterwards, the moment at time  $t = \infty$  is something between moments  $M_0$  and  $M_1$  (dotted line)
- 4) In the time period  $t_0 \dots \infty$  the moment varies in the hatched area

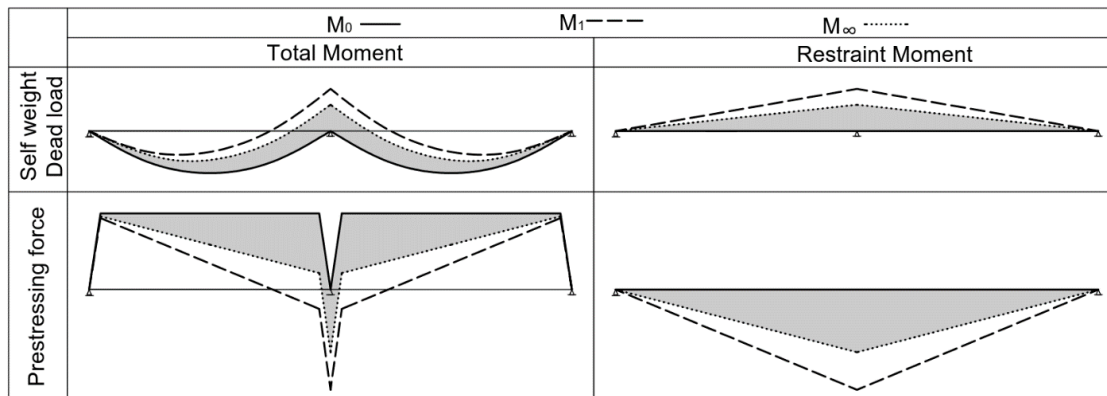


Figure 1 – Typical redistribution of self weight, dead load and prestressing force due to creep in a simple-span structure made continuous.

At the lower half of Fig 1, the same process is presented for the same structure's prestressing force. Prestressing force with constant eccentricity is applied to both beams separately at prefabrication factory. At time  $t = t_0$ , the simple-span prestressing moment is constant apart from the transmission lengths of the prestress force near the ends of the beam. If the prestressing force caused by a straight tendon layout would be adjusted to a two-span structure, the secondary moment of the prestress force would change the total moment  $M_0$  to  $M_1$ . Again, when the static system is changed after the application of the prestress force, the final moment is somewhere between moments  $M_0$  and  $M_1$ . How strongly the moment approaches the monolithically calculated value depends on the concrete's properties and the time when the girders are connected.

The equations presented in this paper are only theoretically exact for a linear creep law if the creep properties are the same in all cross-sections. In general, the error inherent in this assumption is small. In order for the linear creep law to be valid, concrete stress under quasi-permanent loads should not exceed  $0.45f_{ck}(t)$  [13].

Creep distribution effects at time  $t$  may be calculated for structures that undergo changes in a static system using Trost's AAEMM. The basic procedure is to calculate the distribution

moments before the support conditions are changed, and then recalculate the distribution of moments with all dead loads and prestressing force, assuming that the structure was constructed monolithically. The actual long-term redistribution moment for creep can then be found between these two moments, according to Eq. (9) [13, 14, 22].

$$S_t = S_0 + (S_c - S_0) \frac{E_c(t_c)}{E_c(t_0)} \frac{\varphi(t, t_0) - \varphi(t_c, t_0)}{1 + X\varphi(t, t_c)} \quad (9)$$

where

- $S_0$  is the internal forces at the end of the construction process before support conditions are changed
- $S_c$  is the internal forces that are obtained if the structure is constructed monolithically
- $t_0$  is the age of the application of the load
- $t_c$  is the age of the concrete when the support conditions are changed
- $\varphi(t, t_0)$  is creep coefficient at time  $t$  for concrete age  $t_0$  at time of first loading
- $\varphi(t_c, t_0)$  is creep coefficient at time  $t_c$  for concrete age  $t_0$  at time of first loading
- $\varphi(t, t_c)$  is creep coefficient at time  $t$  for concrete age  $t_c$  at time of first loading

### 3.5 Restraint moment due to differential shrinkage

If bond between composite structures deck and beam part is sufficient, differential shrinkage causes deflection to the composite deck-girder system. For a continuous structure, deflection is prevented at the intermediate support, and this causes a negative restraint moment as indicated in Fig 2. EN 1992 does not include this phenomenon [6, 8].

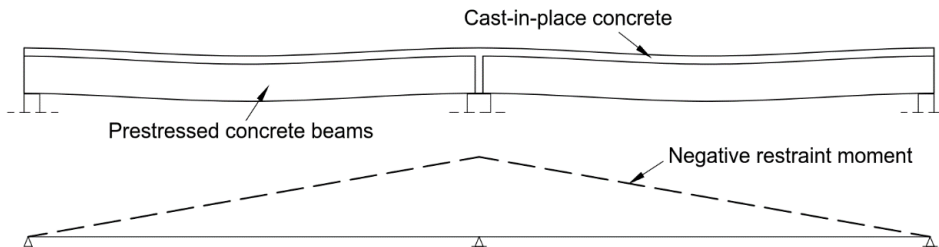


Figure 2 – Deformation and the resulting restraint moment due to differential shrinkage in a composite continuous structure.

In most of the methods used, the compressive internal force produced by the shrinkage difference between the slab and the girder is defined as

$$N_c = \Delta\epsilon_{cs} A_d E_{cm} \quad (10)$$

where,

- $\Delta\epsilon_{cs}$  is  $\epsilon_{csslab}(t) - (\epsilon_{csbeam}(t) - \epsilon_{csbeam}(t_0))$
- $\epsilon_{csslab}(t)$  is shrinkage strain in CIP slab at time  $t$
- $\epsilon_{csbeam}(t)$  is shrinkage strain in prestressed member at time  $t$
- $\epsilon_{csbeam}(t_0)$  is the shrinkage in prestressed member that has developed before casting the slab
- $A_d$  is cross-sectional area of CIP slab

$E_{cm}$  is modulus of elasticity of CIP concrete

This compressive force causes constant moment  $M_{cs}$  to the cross-section

$$M_{cs} = N_c z_{cp} \quad (11)$$

where

$z_{cp}$  is distance between mid-depth of CIP slab and centroid of the composite section

The restraint moment due to differential shrinkage depends strongly on the cross-sectional area of the deck slab  $A_d$  in Eq. (10). In bridge structures the girders are located near each other, and it is reasonable to presume that the effective width of the slab includes the entire distance between girders. In building structures, on the other hand, the beams are further away from each other, which might affect the cross-sectional area of the deck in Eq. (10). This matter is discussed in Sections 4.3 and 5.3. The amount of differential shrinkage also depends on girder age at continuity. If the girders are rather old, the strain difference between the slab and the girders is supposedly larger and negative restraint moment increases. On the other hand, if the girders are young when they are connected, the moment caused by differential shrinkage is smaller if the slab and the beam are assumed to shrink at the same rate.

Statically indeterminate internal moment  $S_{sh}$  caused by differential shrinkage in a perfectly elastic structure can be determined with the Force Method, for example. Secondary moments caused by differential shrinkage develop gradually with time. Because of that, they are reduced by creep. The actual statically indeterminate internal moment  $S_{sht}$ , at time  $t$ , including the relaxation due to creep, is then given by Eq. (12) [11].

$$S_{sht} = \frac{S_{sh}}{1 + X \varphi(t, t_0)} \quad (12)$$

where

$t_0$  is the time when the curing of the deck ended  
 $X$  is the ageing coefficient which may be considered equal to 0.8 for long-term calculations

Data from various field tests indicate that the effects of differential shrinkage do not materialise. Therefore it is questionable if the methods used to analyse it are correct. It has even been proposed that differential shrinkage can be ignored in the design phase [3, 23].

### 3.6 Restraint moments in design

Restraint moments are generally taken into account in serviceability conditions. In some cases restraint moments may reduce the total moment of the structure. According to Ref. [3], restraint moments shall not be included in combinations in these situations. Consideration of the restraint moments can often be ignored at the ultimate limit state if there is sufficient rotation capacity available to shed the restraint moments [3, 22].



## 4. RESEARCH METHODS

### 4.1 Literature review

A literature review on the continuity of precast, prestressed concrete beams with CIP decks and time-dependent deformations of concrete was conducted. Literature published between 1961 and 2018 was collected and reviewed. The literature review was conducted for the purpose of finding methods of evaluating restraint moments in simple-span girders made continuous with CIP decks. The study also focused on exploring design specifications and standards of different areas concerning this topic. The overview of the literature review is presented in Chapter 3 of this article.

### 4.2 Experimental study

The goal of the experimental study was to explore the shrinkage and creep properties of conventional Finnish types of concrete used in precast, prestressed beams and CIP slabs. According to RILEM recommendations, creep and shrinkage strain measuring should be performed on cylinder specimens. In this study, it was decided that tests on beam samples would be carried out so that the results would be as analogous as possible to the studied structure. For the experimental programme, six rectangular ( $300 \times 300 \text{ mm}^2$ ) beams were tested for time-dependent strains. Two of the test beams, B1-sh and B1-cr, represent the composite structures beam part, and the remaining four test specimens, B2-sh, B2-cr, B3-sh and B3-cr, represent the slab part. Half of the test specimens are for creep measuring (cr) and the other half are for the shrinkage test (sh). For creep specimens, the sustained load was applied with concentrated prestressing force. Table 1 displays general data of the beams. Test specimens were stored in the laboratory for 3 to 6 months. Average temperature and relative humidity (standard deviation of observed data) at the laboratory during test was  $T = 22.5^\circ\text{C}$  ( $s = 3.3^\circ\text{C}$ ) and  $\text{RH} = 34\%$  ( $s = 12.4\%$ ).

*Table 1 – General information of the shrinkage and creep test beams.*

Beam Mark	Concrete Type	Prestressed or not	Length of specimen [mm]	Date of Casting
B1-sh	SCC (Mix-1)	NO	2,000	22/02/18
B1-cr	SCC (Mix-1)	YES	3,000	22/02/18
B2-sh	OC (Mix-2)	NO	2,000	15/05/18
B2-cr	OC (Mix-2)	YES	4,000	15/05/18
B3-sh	OC (Mix-3)	NO	2,000	12/06/18
B3-cr	OC (Mix-3)	YES	4,000	12/06/18

#### *Concrete mixtures*

Three mixtures were selected for the test in an attempt to simulate the type of Finnish concrete that is usually used in precast, prestressed element fabrication (Mix-1) and CIP deck-structures (Mixes 2 and 3). The mix proportions for the three mixtures tested are presented in Table 2. As mentioned in Section 3.1, SCC is the concrete type that is used most in Finnish precast, prestressed beams. For that reason, Mix 1 representing the composite structures beam part was selected to be SCC. The strength class of Mix 1 was C50/60. Mixes 2 and 3 were ordinary concrete, and the strength class for them was C35/45. Beams B2 and B3 were cast on different

days, and the concrete for them was ordered from a batching plant. Because of that the mixtures differ for test specimens B2 and B3.

*Table 2 – Concrete mixture proportions*

No. of Mix	W/C	W/B	Max Aggr. Size	Fine Aggr. < 6mm	Coarse Aggr. > 6mm	Water [kg/m <sup>3</sup> ]	Cement [kg/m <sup>3</sup> ]	Fly Ash [kg/m <sup>3</sup> ]	Aggr. [kg/m <sup>3</sup> ]	Air-Pro V5
<b>Mix-1 (SCC)</b>	0.418	0.366	12mm	63%	37%	177	423.5	59.6	1732.5	0%
<b>Mix-2 (OC)</b>	0.450	0.450	16mm	56%	44%	184.5	410	0	1692	0.03%
<b>Mix-3 (OC)</b>	0.393	0.393	16mm	55%	45%	171	436	0	1704	0.03%

In its plastic state, self-consolidating concrete has high flowability and good segregation resistance, and it doesn't require vibration. These special properties are attained by using admixtures and increasing the total quantity of fines in concrete. Greater fines content can be achieved by increasing the content of cementitious materials or integrating mineral fines. From Table 2, it can be seen that Mix-1 has higher paste volume, less coarse aggregate and a higher fine-coarse aggregate ratio than OC Mixes 2 and 3 [24].

#### *Manufacturing and prestressing*

Test beams B1-sh and B1-cr were produced in a prefabrication factory's prestressing bed. The strand pattern used for the B1 beams is shown in Fig. 3. The tensile stress in strands was 1400 MPa, and it caused uniform compression stress ( $\sigma_c = 5.9$  MPa) to the cross-section after release. The tendon force was launched to the beams 12 hours after casting. The curing of the girders with a plastic foil shield was discontinued at the same time. For beam B1-sh all the strands were debonded along their length so that they stayed non-prestressed. Deponding was successfully verified with strain gauge measurements during prestress launching. The beams were transported to the laboratory of TUT on the same day they were prestressed.

Test beams B2-sh, B2-cr, B3-sh and B3-cr were cast in the laboratory. Prestressing was launched into the creep test beams by post-tensioning with the Dywidag strand technique. The tensile stress in strands was about 1250 MPa, hence it caused the same uniform compression stress to the cross-section after the slip at the anchorages as the prestress in test beam B1-cr. Reinforcement of the beams is shown in Fig 3. The beams were covered with plastic foil right after casting. The foil was removed after a week, which was assumed to be the conventional curing time for CIP slabs in site conditions. After the removal of the foils the creep test specimens were prestressed.

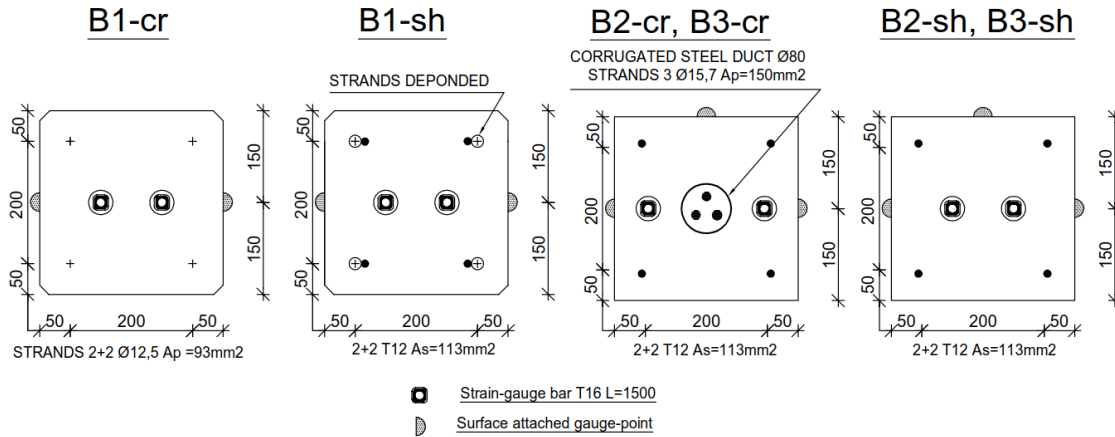


Figure 3 – Test beams' cross-section details and strain gauge locations.

#### Strain gauge and gauge-point measurements

The strain in test beams was measured with strain gauge bars. Each beam contained two strain gauge bars so that each specimen gave two independent sets of data. A strain gauge bar consists of a reinforcing bar ( $\text{Ø}16\text{mm}$ ,  $f_{yk} = 500\text{ MPa}$ ,  $L=1,500\text{ mm}$ ), strain gauges, shielding materials and wires. In this arrangement the strain gauge exhibits the same deformation as the surrounding concrete. The deformation data were saved every second during prestressing and once an hour during the long-term tests that lasted from two to four months. In addition to strain gauge measurements, surface-attached gauge-point measurements were made in order to secure the validity of the strain gauge measurements.

#### Modulus of elasticity test

Cylinder specimens ( $d=150\text{ mm}$ ,  $h=300\text{ mm}$ ) were fabricated for each batch of concrete. The specimens were stored and cured next to the B1, B2 and B3 beams in order for their condition to be as similar as possible. The testing procedure of the SFS EN 12390-13 standard was applied to determine the stabilised elastic modulus of the specimens. The elastic moduli of concrete were measured at ages 7, 28, 90 and 180 days. In addition, the elastic deformation of beams B1-cr, B2-cr and B3-cr was measured in the prestressing phase with strain gauge bars. The modulus of elasticity at loading was then defined according to the measured elastic strain and known prestressing force [25].

### 4.3 Analytical study

An analytical tool has been developed to predict restraint moments according to equations presented in Chapter 3. The tool takes into account the creep and shrinkage effects, prestress losses, age at loading and the construction sequence. Prestress losses are calculated according to Eurocode equations. In the tool it is possible to use two different deformation properties. Elastic modulus, shrinkage and creep coefficient are assumed as being according to EN 1992-1-1 or experimental tests made in this study. In Chapter 5, the results are presented in an example structure with both deformation properties, and the results are compared.

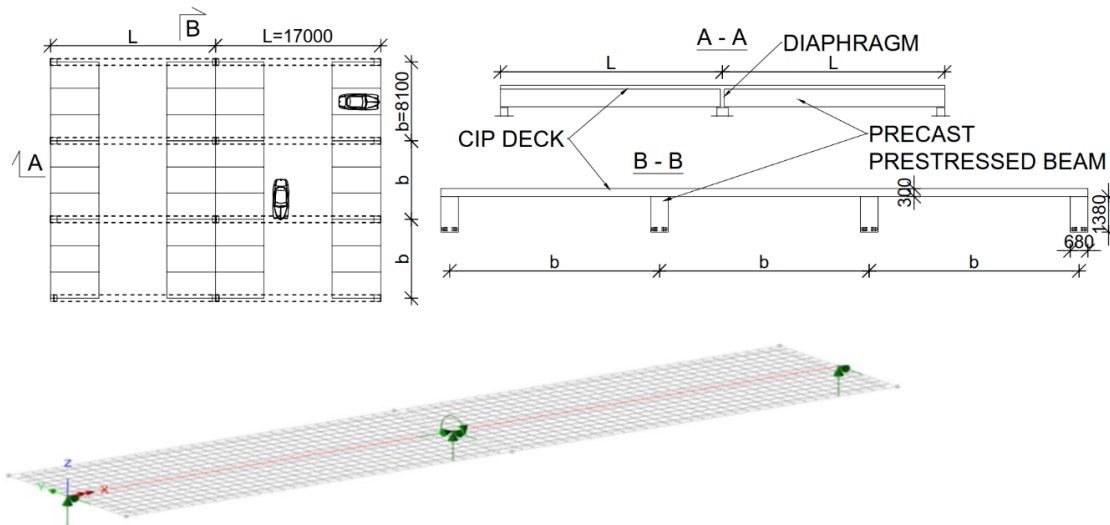


Figure 4 – Example parking deck structure and structural model from LUSAS.

In the analytical study, the example structure (Fig. 4) was a composite beam composed of rectangular beams ( $b \times h = 0.68 \times 1.38 \text{ m}^2$ ) and a CIP slab ( $h = 0.3 \text{ m}$ ). The distance between the beams was 8.1 m. Two simple-span beams (span length 17 m) were made continuous with the CIP slab. The prestressing force in the beam was 6 MN and eccentricity from the cross-section's soffit was 0.12 m. The ages of the girder when continuity was established were 7, 14, 28 and 90 days. Dimensions and other variables of the example structure were in accordance with a typical parking deck structure.

Shrinkage and creep experimental data ended at 90...130 days depending on the test sample. Future deformations are predicted, therefore restraint moments could have been determined for a more distant time. The principles used in the extrapolation are explained in Sections 5.1 and 5.2. The size difference between the studied structure and the test samples is taken into account with EN 1992-1-1 formulas (3.10), (B.3) and (B.7). In the experimental study, the beam concrete's creep coefficient is determined only for the case where the time of loading is 12 hours. In the analytical study, the beam's measured creep coefficients are also needed for loading ages of 7, 14, 28 and 90 days. These coefficient values are determined with the help of measured data from 12-hour loading and EN 1992-1-1 expression (B.5) [9].

Equations (9) and (12) are based on the assumption that there is only a single value for the structures' creep coefficient. In reality, the CIP deck and the beam have their own material properties. In the analytical tool, the beam's creep values are used for Equation (9) and the deck's creep coefficient for Equation (12) according to reference [21].

#### *Effective width for differential shrinkage*

Every reference document found about this theme used the slab's whole width to determine axial force produced by differential shrinkage. In building structures the beams are located relatively far from each other compared to bridges, and this should be taken into account in the cross-sectional area of the deck in Eq. (9). Computational check was made with the finite element analysis software LUSAS to determine composite structures' effective width for loads produced by differential shrinkage. The results of this study were implemented in the analytical tool [21,26].

## 5. RESULTS AND DISCUSSION

### 5.1 Shrinkage and creep test results

Beam and deck shrinkage and creep strains were tested in the experimental phase of this study. The procedures and methods of measuring the strains have been presented in Section 4.2. The strain gauge and gauge-point measurements yielded congruent results for the B1 samples. A minor change in the preparation of strain gauge bars used in samples B2 and B3 caused inaccuracy to strain gauge measurements. This inaccuracy was improved by calibrating the strain gauge measurement values with parallel gauge-point measurements. For the sake of clarity, only strain gauge measurements are presented in this paper.

Figures 5 and 6 show the progress of shrinkage strains for the beam and deck concrete with the passage of time. The progress of both strains has been drawn according to EN 1992-1-1 and experimental data. The experimental data ends at three to four months. The logarithmic trend line is fitted to the experimental data to illustrate the mathematical form of measured shrinkage. The trend line formula and R-squared value, which describe the exactness of the model, are displayed in the chart. The shrinkage prediction beyond the test period is made according to test data and EN 1992-1-1 formulas (3.9) and (3.13).

The autogenous shrinkage can be distinguished from the total shrinkage for the measurements taken of the deck samples B2-sh and B3-sh, which were cured for a week. The shrinkage that happened during curing was assumed to be autogenous shrinkage. In beam sample B1-sh the curing duration was so short (12 hours) that autogenous shrinkage could not be discerned. When predicting beam shrinkage, the autogenous part of measured shrinkage has to be assumed to be in accordance with Eurocode.

From Fig. 5 it can be seen that the shrinkage strains measured from the sample made from Mix 1 (SCC) follow quite accurately the strains calculated according to Eurocode. On the other hand, the difference between measured strains and shrinkage, according to Eurocode for Mixes 2 and 3 (OC) presented in Fig. 6, is considerable. According to experimental data, shrinkage for conventional C35/45 deck concrete is about 40% less than Eurocode predicts. It can also be seen that two different deck shrinkage test samples yield very similar results, although the concrete mixtures were not exactly the same. This measured data exceeds the shrinkage variation  $\pm 30\%$  defined in EN 1992-1-1 [2, 9].

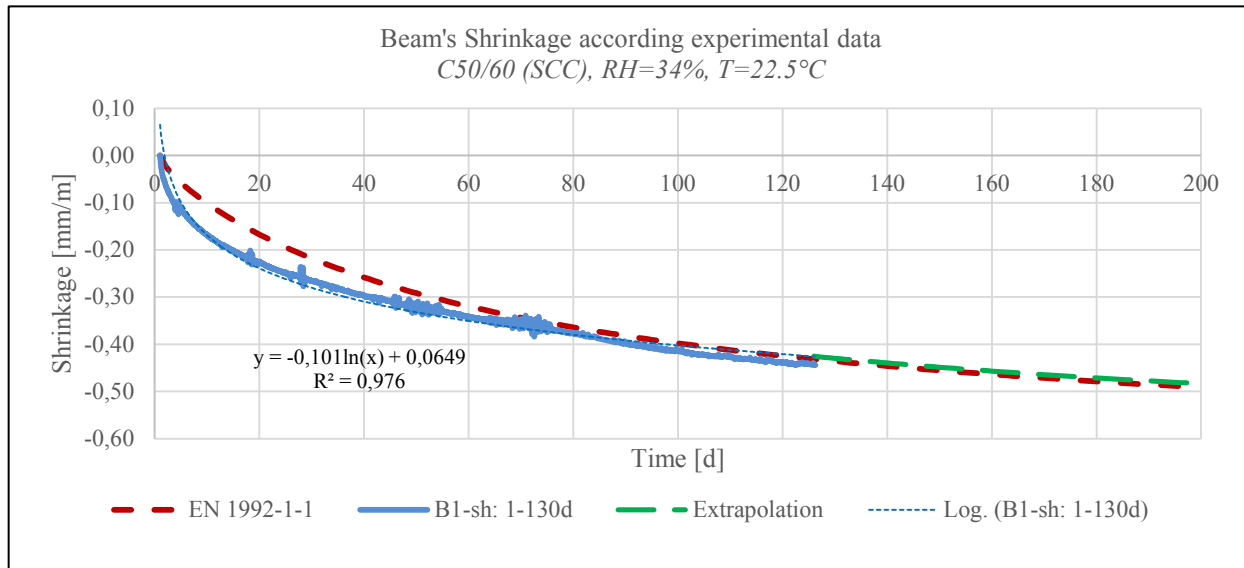


Figure 5 – Beam shrinkage according to experimental data (B1-sh) vs EN 1992-1-1.

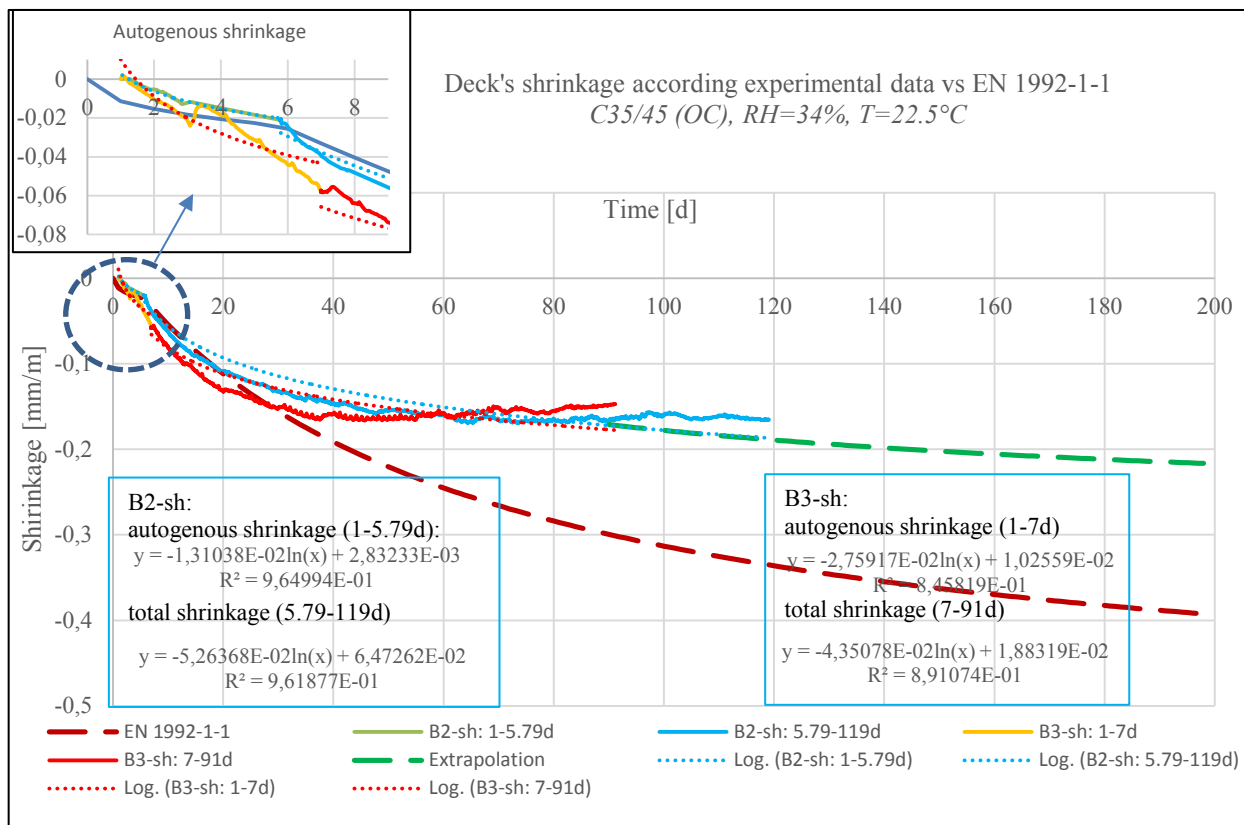


Figure 6 – Deck shrinkage according to experimental data (B2-sh, B3-sh) vs EN 1992-1-1.

Shrinkage values of different parts of the the cross-section are interesting in this study, because their difference causes restraint moments. It is generally understood that the precast beam in the composite concrete section has completed a significant part of its total shrinkage by the time the deck is cast, so the deck slab will shrink by a relatively greater amount and cause axial force and sagging moment into the composite section. This then causes negative restraint moments into the statically indeterminate structures. This happens if the beam and deck shrinkages are

supposed to develop according to Eurocode formulas. However, the results of the experimental study show that the deck OC's shrinkage is so minor compared to the beam SCC's shrinkage that differential shrinkage changes the sign and starts bending the structure upwards. This indicates that, with these concrete mixtures, differential shrinkage could cause positive restraint moments to the statically indeterminate composite structures instead of negative moments.

Figures 7 and 8 show the development of the creep coefficient for the beam and deck concrete. The development of both factors has been drawn according to EN 1992-1-1 and experimental data. The creep strain is obtained by subtracting the tested shrinkage strain (B1-sh, B2-sh and B3-sh) from the total strain measured from the creep specimens (B1-cr, B2-cr and B3-cr). Also, with the creep test the logarithmic trend line is fitted to the experimental data to illustrate the mathematical form of the measured creep coefficient factor. The creep growth prediction after the end of the data is made according to EN 1992-1-1 and formula (B.7) [9, 26].

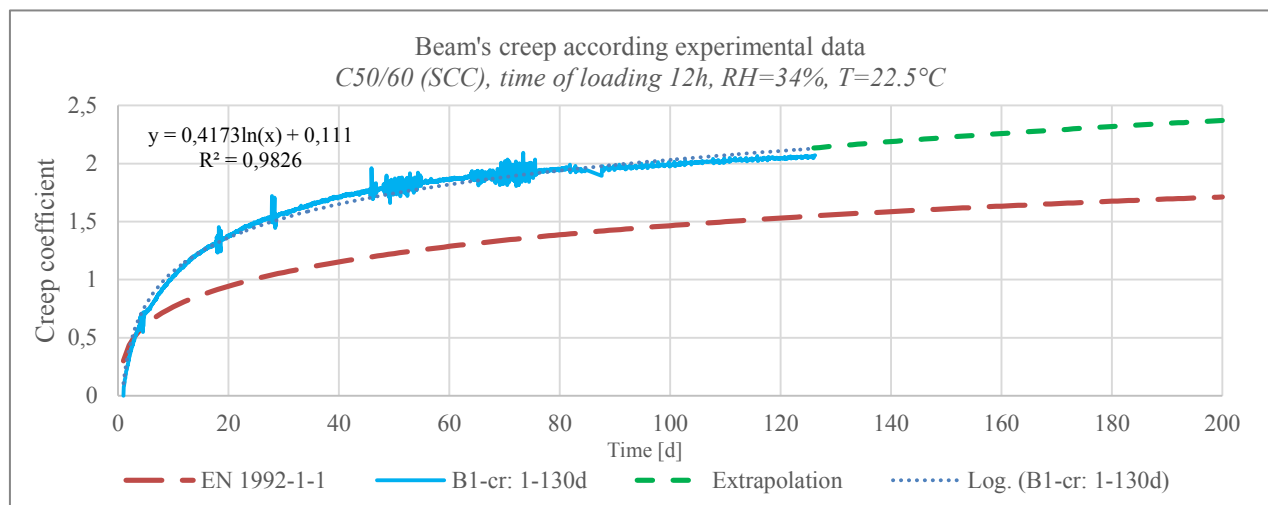


Figure 7 – Beam creep according to experimental data (B1-cr) vs EN 1992-1-1.

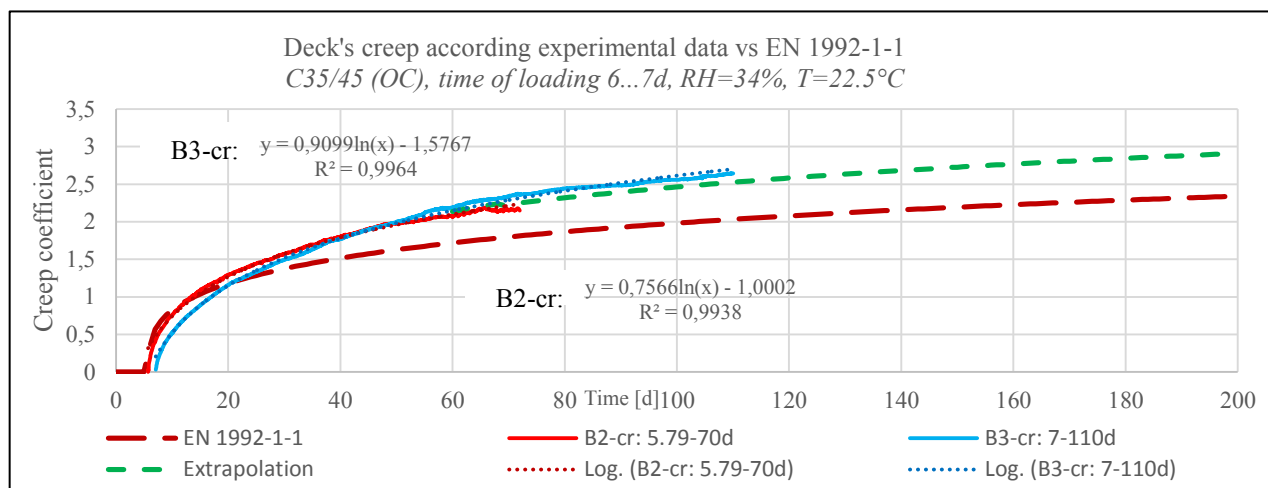


Figure 8 – Deck creep according to experimental data (B2-cr, B3-cr) vs EN 1992-1-1.

From Figure 7, it can be seen that the creep coefficient measured from the test beam made from SCC is about 40% higher compared to the creep coefficient calculated according to Eurocode. The result was anticipated, because many references state that SCC's high paste content causes higher creep deformations than that of OC of equal strength. This measured data exceeds the

creep variation  $\pm 20\%$  defined in EN 1992-1-1 [2, 9]. Also the OC deck seems to creep more than Eurocode models would predict. Fig. 8 indicates that the creep strains of deck concrete test beams are about 20% higher than Eurocode models predict. Once again it is clear that two different deck creep test beams yield similar results, although the concrete mixtures were not exactly the same. When the beam's creep coefficient factor grows, the restraint moment for creep increases at the same time. Deck's higher creep factor increases the release of restraint moments caused by differential shrinkage.

The experimental test was conducted in the structural engineering laboratory in TUT, where relative humidity is quite dry (34%) compared to RH values commonly used in the design phase. This may cause a source of error to the conclusions made from this study. On the other hand, one main topic of interest in the study is the comparison of the properties of the two materials with each other. Such an experiment is also possible in a dry climate, because the condition is the same for both materials. The experimental test lasted three to four months, which is a short time compared to the structure's service life of 50-100 years. Then again, according to Eurocode a significant part (55-70%) of creep and shrinkage has developed during the testing period. Based on that, it is possible to make quite reliable models according to available data [9].

## 5.2 Modulus of elasticity test results

Figure 9 shows  $E_{cm}$  development for beam and deck concrete. In the plots it has been drawn both modulus according to EN 1992-1-1 and experimental tests. Measured compressive strength values are also added to the figure. It can be seen that the testing of both types of concrete has yielded lower elastic modulus values than EN 1992-1-1 would predict. The tests indicate that the elastic modulus of the concrete types was 10 to 15% lower compared to the Eurocode values. The beam concrete's measured data showed a growth in the elastic modulus with time, and it was possible to fit the logarithmic trend line to data points in the time period  $t_0 \dots 180d$ . After that the beam's elastic modulus is assumed to be constant. The deck's test values had such a large variance that the modulus time dependence was selected to represent as a constant average after 7 days. Different elastic modulus time dependence and lower modulus values increase prestressing losses and affect restraint moments.

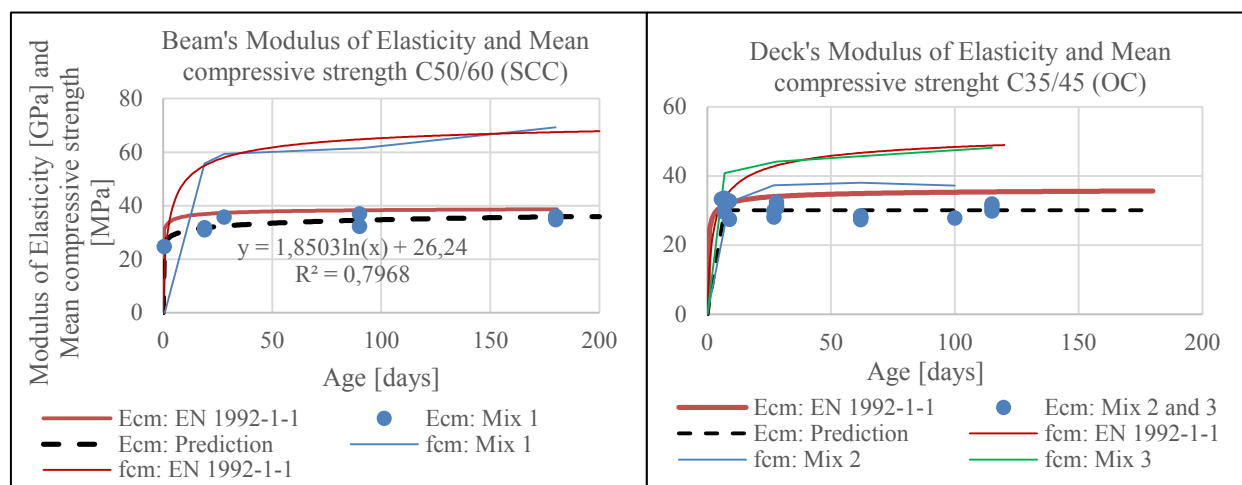


Figure 9 – Elastic modulus and mean compressive strength of tested concrete according to experimental data (Mix 1, 2 and 3) vs EN 1992-1-1



### 5.3 Effective width variation for differential shrinkage

Composite structures restraint forces produced by differential strains were determined with the finite element analysis software LUSAS. Forces calculated with LUSAS were compared to hand-calculated forces which were determined under the assumption that the width of the whole slab was effective in determining axial force. The effective width for differential shrinkage loading, determined according to the LUSAS analysis regarding the selected parking garage top deck structure, was 95% of the whole deck width. The amount or direction of the shrinkage load has no effect on the effective width. A noteworthy observation made from this simple study was that the usage of effective width of flanges determined with Eurocode formulas yields results that are clearly too small in this loading type.

### 5.4 Time-dependent restraint moments in example structure

Example structures' calculated restraint moments developed in time in the centre support with two different material models are plotted in Figure 10. Negative restraint moments produce tension to the diaphragm's top side, while positive restraint moments seek to crack the diaphragm's soffit.

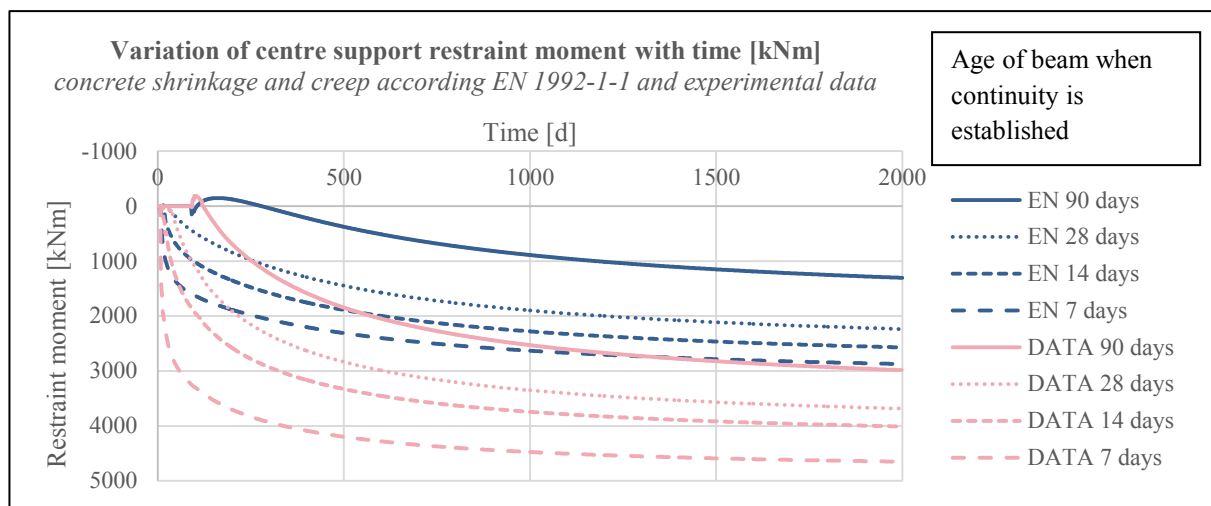


Figure 10 – Variation of example structures' (Fig. 4) centre support restraint moment with time according to EN 1992-1-1.

The blue lines in the figure represent restraint moments calculated with Eurocode material models. The shape of the Eurocode set of curves is similar to time-dependent restraint moment diaphragms presented in earlier studies made from this topic [13, 27]. If the age when continuity is established is young, the shrinkage difference between the slab and the beam is small and the negative moment produced by differential shrinkage is likewise small. In this case, the positive restraint moment grows the most. On the other hand, when the beam is older when connected for continuity, differential shrinkage plays a bigger role and the restraint moments are negative in the first year. In this case the final positive restraint moment remains smaller because differential shrinkage decreases it. For the selected example, the structure soffit's cracking moment is 1 375 kNm if the diaphragm is made from C35/45 concrete. According to the models

of EN 1992-1-1, it can be seen that restraint moments remain under this cracking moment for the first 2 000 days if the beams are 90 days old when connected.

The same analysis is presented for converted material properties with light red lines. In this analysis used shrinkage, creep and modulus of elasticity models are according to experimental data presented in Sections 5.1, 5.2 and 5.3. In the analysis, conducted according to tested material properties, positive restraint moments grow about two times bigger when converted to blue Eurocode curves. This difference results from the deck slab shrinkage test results. According to experimental data, deck shrinkage was so minor that beam shrinkage was more intense in comparison, despite the age of the beam when continuity was established being 90 days. This difference caused an unexpected result, according to which differential shrinkage also causes a positive restraint moment. With these deformation properties, both creep and differential shrinkage cause a positive restraint moment, and the resulting moments are considerably larger. In addition, beams' creep coefficient factor was 40% larger converted to the EN 1992-1-1 model. Beams' larger creep coefficient increases the restraint moments produced from the change in the static system

Field tests conducted by various researchers do not show the effects of differential shrinkage. It has been stated that the problem is not the structural model, because the model seems to give consistent results when evaluating restraint moments caused by temperature difference. It is believed that the problem might instead be the values used for deck shrinkage [3,28]. The experimental data gained from this research supports this claim. This observation is important, because if the differential shrinkage does not resist positive restraint moments as the models predict, the actual positive moments that develop may be worse than predicted.

In Ref. [3], creep and shrinkage restraint moments are allowed to taken to be zero if the girder's minimum age is at least 90 days when continuity is established. According to the analysis made in this study, restraint moments cannot be neglected in this studied example structure even if the minimum age of the precast girder would be extended to three months. This is because experimental data suggests that positive moments are not mitigated by the deck slab shrinkage in the way that the usual design models predict, and the structure is also different. However, as the analysis shows, the older the girder age is when continuity is established, the smaller the resulting restraint moments are.

## 6. CONCLUSIONS

The experimental study showed a notable difference in the tested shrinkage and creep behaviour of selected concrete types compared to Eurocode prediction models. It also proved the need for an experimental study before evaluating restraint moments due to changes in the static system and differential shrinkage. The shrinkage strains measured were 0-40% less than expected and creep strains were 20-40% greater. The tested modulus of elasticity values were 10-15% lower compared to values used in the design.

Restraint moments were calculated with two different concrete deformation properties for the selected parking deck structure. In the example calculation, two simple-span composite beams were made continuous after a period of 7 to 90 days from the beam casting. The magnitude of one parking deck's restraint moments was resolved as a result of this study.

The analysis shows that positive restraint moments grow about two times greater, if tested material properties are used instead of Eurocode creep and shrinkage prediction models. Larger positive restraint moment values result mainly from shrinkage test results, which show that the direction of differential shrinkage restraint moments is opposite compared to the one that was expected. As a result creep and differential shrinkage, restraint moments are additive and the resulting total moment grows considerably.

No appearance of negative restraint moments is in agreement with prior studies, which claim that shrinkage values used computing restraint moments due to differential shrinkage are not correct. The calculation results of this study indicate how sensitive the restraint moments are to the creep and shrinkage models used. It seems that the inaccuracy of design methods for calculating restraint moments increases if the composition of the concrete types used for beam and deck structure differs considerably from each other. If the concrete types used were more similar, the direction of the restraint moments could be easier to predict.

This experimental study was conducted with merely two types of concrete and under one testing condition. In order to gain a more comprehensive understanding of the restraint moments of this kind of structure, more material testing is required. However, according to the results of this study it could be recommendable to accurately define a required concrete composition for the deck and the beam in the design phase so that creep and shrinkage could be better predicted. The use of SCC in the precast beam should be considered in detail. The advanced age of the girder when establishing continuity seems to also have an effect on minimising the restraint moment.

These conclusions have been made according to measurements which have taken three to four months. Long-term measurements of test samples will be continued and more SCC test samples are going to be studied in order to gain more data. The next phase of this study is the evaluation of the effect of restraint moments on the building structure's continuity. Analytical study and physical testing will be conducted to determine the potential of simple-span prestressed beams made continuous in building structures.

Measured shrinkages for deck concrete mixtures 2 and 3 were surprisingly low. Further investigation on these concrete mixes should be made to clarify the reason for small shrinkage test results. The findings of experimental tests made on SCC beams indicate that the creep coefficient is bigger and early age modulus of elasticity smaller than the used design specifications predict. SCC is a widely used material in Finnish prestressed concrete fabrication, but its use isn't taken into account in any way at the design phase. More testing and analysis of SCC's usage in prestressed concrete beams is needed.

## REFERENCES

1. Finnish Concrete Society: "Concrete Textbook 2018, by 201," Vaasa, Finland, 2018, 568 pp. (In Finnish).
2. International Federation for Structural Concrete (fib): "CEB-FIP, Model Code 2010," Final draft, Volume 1, *Bulletin* 65, Switzerland, 2012, 357 pp.
3. American Association of State Highway and Transportation Officials: "AASHTO LRFD Bridge Design Specifications, Customary U.S. Units," Section 5, "Concrete Structures," Washington DC, USA, 2012, 332-589 pp.

4. Miller R A, Castrodale R, Mirmiran A & Hastak M: “NCHRP Report 519, Connection of Simple Span Precast Concrete Girders for Continuity,” *Transportation Research Board*, Washington DC, 2004, 202 pp.
5. Abdalla O A, Ramirez J A & Lee R H, “Strand Deponding in Pretensioned Beams – Precast Prestressed Concrete Bridge Girders with Deponded Strands, Continuity Issues,” Purdue University, West Lafayette, Indiana, USA, 1993, 265 pp.
6. McDonagh M D & Hinkley K B, “Resolving Restraint Moments: Designing for Continuity in Prestressed Concrete Girder Bridges,” *PCI Journal*, July-August 2003, 16 pp.
7. Freyeremuth C L: “Design of Continuous Highway Bridges with Precast, Prestressed Concrete Girders,” *PCI Journal*, April 1969, pp. 14-39.
8. Meyerson R, Weyers R E, Via C E, Mokarem D W & Lane D S: “Evaluation of Models for Predicting (Total) Creep of Prestressed Concrete Mixtures,” Virginia, USA, 2002, 55 pp.
9. “EN 1992-1-1, Eurocode 2: Design of Concrete Structures. Part 1-1: General rules for buildings,” Brussels, Belgium, 2004.
10. Bazant Z: “Mathematical Modeling of Creep and Shrinkage of Concrete,” Chapter 3, “Creep Analysis of Structures,” Chichester, New York, Brisbane, Toronto, Singapore, 1988, pp. 217-273.
11. ACI Committee 209: “Publication SP-76, Design for Creep & Shrinkage on Concrete Structures,” Chapter SP76-10, “Prediction of Creep, Shrinkage and Temperature Effects in Concrete Structures”, Detroit, USA, 1982, pp. 193-300.
12. Menn C: “Prestressed Concrete Bridges”, Basel, Boston, Berlin, 1990, 546 pp.
13. “EN 1992-2, Eurocode 2: Design of Concrete Structures. Concrete Bridges. Design and Detailing Rules,” Brussels, Belgium, 2005.
14. “EN 1992-2:2005/AC, Eurocode 2: Design of concrete structures. Concrete bridges. Design and Detailing Rules,” Brussels, Belgium, 2008.
15. Trost H: “Creep, Relaxation and Shrinkage of Structural Concrete,” *IABSE reports*, Switzerland, 1991, Vol. 62, pp. 59-76.
16. Trost H: “Auswirkungen des Superpositionsprinzips auf Kriech- und Relaxationsprobleme bei Beton und Spannbeton,” *Beton- und Stahlbetonbau* (Berlin – Wilmersdorf), No. 10, 1967, pp. 230-238 (in German).
17. Bazant Z: “Prediction of Concrete Creep Effects Using Age-Adjusted Effective Modulus Method,” *Journal of the American Concrete Institute*, Vol 69, 1972, p.p 212-217
18. CEB: “Structural Effects of Time-Dependent Behaviour of Concrete,” *Bulletin* No. 215, Lausanne, Switzerland, 1993, 308 pp.
19. Keitel H: “Selecting an Advanced Creep Model or a Sophisticated Time-Integration? A new Approach by means of Sensitivity Analysis,” *International Journal of Mathematical and Computational Sciences*, Vol. 6, No. 7, 2012, pp. 724-731
20. International Federation for Structural Concrete (fib): “CEB-FIP, Model Code 2010,” Final draft, Volume 2, *Bulletin* 66, Lausanne, Switzerland, 2012, 377 pp.
21. Tadros M K, Girgis M A, Tuan C Y & Alex A A: “Simplified Design for Positive Restraint Continuity Moment in Bridge Girders.” *PCI Journal*, July-August 2018, pp. 62-78.
22. Hendy C R & Smith D A: “Designer’s Guide to EN 1992-2, Eurocode 2: Design of Concrete Structures. Part 2: Concrete Bridges,” London, UK, 2007, 196 pp.
23. ACI Committee 209: “Publication SP-76, Design for Creep & Shrinkage on Concrete Structures,” Chapter SP76-13, “A Simple Method to Analyse Time-Dependent Forces Developed in Continous Concrete Structures” Detroit, USA, 1982, pp. 325-339

24. Betonikeskus Ry: “SCC – Self Consolidating Concrete,” Loviisa, Finland, 2004. (In Finnish).
25. “EN 12390-13, Testing Hardened Concrete, Part 13: Determination of Secant Modulus of Elasticity in Compression,” 2013.
26. Tia M, Liu Y & Brown D: “Modulus of Elasticity, Creep and Shrinkage of Concrete,” University of Florida, USA, 2005, 185 pp.
27. Mattock A H: “Precast-prestressed concrete bridges 5, Creep and Shrinkage studies,” *Journal of the PCA Research Laboratories*, Vol 2, No. 2, 1961, pp. 32-66.
28. Mirmiran A, Kulkarni S, Castrodale R, Miller R & Hastak M: “Nonlinear Continuity Analysis of Precast, Prestressed Concrete Girders with Cast-in-Place Decks and Diaphragms,” *PCI Journal*, September-October 2001, pp. 60-80.